Neuro-Oncology Advances

8(1), vdag159, 2026 | https://doi.org/10.1093/noajnl/vdag159 | Advance Access publication June 12, 2026

Multi-threshold volumetric ^{18}F-FET PET for tumor detection and prognosis in primary glioma

Thura Tun Oo[†], Shaun D. Grega[†], Nathaniel J. Smith, Tristan K. Deaton, Keith G. Ciantar, Wendy Territo, Lu Mao, Sharon Sidenbender, Jesus A. Ocana, Matthew E. Larson, Mark Tann, Kathryn Nevel, Brian D. Graner, Gary D. Hutchins, Mark A. Green, Philipp Lohmann, and Michael C. Veronesi

All author affiliations are listed at the end of the article

Corresponding Author: Michael C. Veronesi, MD, PhD, Department of Radiology, University of Wisconsin, School of Medicine and Public Health, E1/374 Clinical Sciences Center, 600 Highland Avenue, Madison, WI 53792-3252, USA (mveronesi@wisc.edu).
[†]These authors contributed equally to this work.

Abstract

Background. Amino acid PET with ^{18}F-fluoroethyltyrosine (^{18}F-FET) complements MRI to improve specificity of tumor detection. We evaluated whether threshold-based volumetric metrics (TBRthres) provide complementary diagnostic and prognostic information to single-voxel tumor-to-brain ratio maximum (TBRmax).

Methods. This retrospective single-institution study included 100 previously treated glioma patients (WHO Grade 2-4) who underwent ^{18}F-FET PET/MRI (N=96) or PET/CT (N=4) following equivocal findings of tumor progression versus treatment-related changes. Patients received 693.8±79.6 MBq of ^{18}F-FET, with PET analysis based on the 20-40 minute averaged static sequence acquired post-injection. Diagnostic performance, reproducibility, and survival associations were assessed using ROC analysis, intraclass correlation coefficients (ICC), and Cox proportional hazards models.

Results. TBRthres map generation was highly reproducible (ICC > 0.86) and significantly associated with overall survival in univariate analyses (HR range: 3.07-4.45). Volumetric metrics demonstrated diagnostic performance comparable to TBRmax (AUC up to 0.91). TBRmax showed moderate correlation with tumor volume ($R^2 \approx$ 0.35-0.40), indicating partially overlapping but non-redundant information. In multivariate models adjusting for clinical covariates, neither volumetric metrics nor TBRmax remained statistically significant. However, in models adjusting for TBRmax, volumetric TBRthres metrics remained significantly associated with survival. Combined models improved predictive performance at selected thresholds, particularly TBRthres ≥ 1.6 (AUC 0.62 to 0.70, P=.009) and TBRthres ≥2.0 (AUC 0.62 to 0.72, P=.019), with smaller improvement at TBRthres ≥ 2.5.

Conclusion. Volumetric ^{18}F-FET PET metrics provide reproducible measures of tumor burden with diagnostic and prognostic performance comparable to TBRmax. They offer complementary information and, at selected thresholds, modest incremental predictive value beyond TBRmax.

Key Points

- Volumetric TBRthres shows high reproducibility (ICC > 0.86).
- Volumetric metrics show diagnostic performance comparable to TBRmax.
- Combined models improve prognosis at selected thresholds.

Received October 31, 2025; accepted June 8, 2026.

Importance of the Study

Amino acid PET, including with ^{18}F-fluoroethyltyrosine (^{18}F-FET), is recommended as complementary to magnetic resonance imaging (MRI) with the goal of increasing specificity of tumor detection. However, ^{18}F-FET PET tumor-to-brain ratio (TBR) metrics often rely on finding the maximum single voxel TBR (TBRmax) as a key indicator of tumor presence, which is resolution-dependent and may not reflect total tumor burden. In this study, we evaluated whether threshold-based volumetric PET metrics (TBRthres) provide additional diagnostic and prognostic information beyond single-voxel TBRmax. We demonstrate that volumetric TBRthres mapping is highly reproducible and provides diagnostic and prognostic performance comparable to TBRmax while capturing partially non-redundant information related to tumor burden. Importantly, selected volumetric thresholds provided modest incremental predictive value when combined with TBRmax, supporting a complementary rather than universally superior role for volumetric PET analysis in glioma imaging. These findings support further prospective evaluation of integrated volumetric and single-voxel PET approaches for improving clinical assessment of glioma patients.

Amino acid positron emission tomography (AA PET) is recommended by international working groups as a complementary imaging modality along with MRI for the management of patients with glioma.[1] AA PET leverages increased amino acid transport in glioma cells, resulting in high tumor-to-background contrast and improved specificity for viable tumor tissue, particularly in regions where MRI findings are equivocal.[2,3] This property makes AA PET a clinically useful adjunct to MRI rather than a replacement. Unlike ^{18}F-FDG PET, amino acid tracers show low physiological uptake in normal brain, supporting their clinical use for distinguishing tumor progression of disease (POD) from non-tumoral treatment-related changes (TRCs).[2,4] However, commonly used static PET metrics based on maximum and mean uptake values may provide incomplete information regarding the full extent of metabolically active tumor,[5-8] motivating the evaluation of volumetric approaches.

O-(2-^{18}F-fluoroethyl)-L-tyrosine (^{18}F-FET) is the most widely studied AA radiotracer in Europe and other countries[9-12] and is under active application for FDA approval in the United States. The biological basis of AA PET relies on L-type amino acid transporter 1 (LAT1, SLC7A5), which is upregulated in glioma cells to support protein synthesis and metabolic demand,[13-15] and ^{18}F-FET uptake is therefore presumed to be transported predominantly via this mechanism. However, direct evidence for LAT1-mediated transport of AA PET tracers in vivo remains limited, and a recent study found no correlation between LAT1 expression and uptake of ^{18}F-FET or ^{11}C-methionine in infiltrating glioma in a subset of patients.[16] Despite this uncertainty, amino acid PET is thought to occur independently of blood-brain barrier disruption,[17] enabling AA PET tracers to detect metabolically active tissue beyond regions of contrast enhancement.[18-20]

Among the static metrics for ^{18}F-FET PET interpretation, the tumor-to-brain-ratio maximum and mean (TBRmax and TBRmean) acquired from the 20-40 minute period after injection are the most widely studied and utilized in clinical practice.[21,22] The TBRmax in particular is a key clinical biomarker but its binary (positive/negative) interpretation at fixed thresholds may lack nuance for borderline values, causing diagnostic uncertainty.[21,23] Importantly, LAT1 is expressed in astrocytes, inflammatory cells, and endothelial cells and can be detected in reactive tumor microenvironments after treatment.[24-27] Following chemoradiotherapy in glioma patients, ^{18}F-FET PET can rarely show increased uptake in treatment-related tissue changes, such as inflammation, gliosis, or radionecrosis, in the absence of viable tumor, leading to false-positive findings in a minority of cases.[5,28] This overlap in PET avidity is largely driven by high LAT1 expression in tumor cells, while reactive tissue may contribute modestly through lower-level LAT1 expression or other mechanisms, providing a biological explanation for the difficulty in distinguishing POD from TRCs. It is important to note that ^{18}F-FET avidity may not exclusively represent viable tumor tissue as ^{18}F-FET uptake reflects transport via LAT-1 and LAT-2 transporters.[29-31] These transports are upregulated in tumor cells but also can be expressed in non-neoplastic tissue.[32,33] We aim to improve this discrimination by capturing not only intensity of uptake but also spatial extent of ^{18}F-FET avidity.

Besides reducing the quantitative tumor assessment to a single voxel of data, TBRmax is inherently dependent on the spatial resolution of the PET system and image postprocessing protocols,[34] limiting the comparability of cutoff values across institutions and scanner platforms.[35] Single-voxel measurements may fail to capture tumor heterogeneity and are susceptible to image noise and varying focal uptake. Furthermore, borderline TBRmax measurements seen in clinical practice create diagnostic uncertainty, as binary interpretation fails to reflect total tumor burden. Therefore, incorporating volumetric parameters is increasingly recognized to improve the reliability of PET interpretation in glioma imaging.[36,37] In addition to efficacy assessment, accumulating research has emphasized the prognostic value of volumetric parameters in newly diagnosed gliomas,[38,39] as well as in recurrent settings.[40,41] While most volumetric studies to date have focused on a single threshold (commonly TBR > 1.6),[42,43] comprehensive analyses and their reproducibility across a range of clinically relevant thresholds remain limited. Moreover, whether threshold-based volumetric analysis provides incremental diagnostic and prognostic value beyond single voxel TBRmax remains unclear.

To attempt to address the limitations in ^{18}F-FET PET interpretation, we retrospectively analyzed 100 patients with confirmed glioma who underwent simultaneous ^{18}F-FET PET/MRI to evaluate whether threshold-based volumetric TBR maps (TBRthres maps) can enhance diagnostic monitoring accuracy and prognostic value compared to a single voxel TBRmax value alone. We hypothesized that adding

volumetric information defined by various TBRthres would contain important diagnostic and prognostic information superior to single-voxel TBRmax information. We assessed inter-rater reproducibility, diagnostic performance across TBR thresholds, and the prognostic relevance of volumetric cutoffs. This single-institution U.S. study aims to establish a clinically actionable framework that integrates tumor volume as an additional informative metric to improve the reliability of ^{18}F-FET PET in recurrent glioma assessment.

Methods

Study Population

Under expanded-access IND #150883, participants underwent ^{18}F-FET imaging after providing written informed consent, with all procedures approved by the Indiana University institutional review board (see Supplementary Data Section for more details). ^{18}F-FET PET/MRI was performed on 100 patients with known primary glioma following equivocal brain MRI that raised concerns about whether the observed changes indicated tumor relapse or were due to nonspecific, non-tumoral TRC. PET imaging commenced as a result of multidisciplinary conference discussions or when the primary neuro-based treating team in their clinical care did not have a definitive diagnosis in further management of the patient at that time. Imaging was interpreted by a board-certified nuclear medicine physician and neuroradiologists. The final report was submitted to the PACS system for incorporation into clinical care management. The outcome, whether POD or TRC was determined by 1 of 2 methods: (1) pathologic confirmation (n=29), based on pathology reports from subsequent surgery or biopsy, which served as the reference standard; or (2) a minimum of 6-month clinical and radiological follow-up (n=71), including post-imaging treatment decisions, follow-up imaging findings, and clinical notes on patient condition. All subsequent imaging, clinical notes, and treatment decisions were then subjected to a consensus panel that included 2 experienced, board-certified neuroradiologists and one nuclear medicine physician for outcome confirmation in the 71 patients (see Supplementary Data for further details).

^{18}F-FET PET

For the imaging study, a total of 100 patients underwent scans after a 4-hour fast and bladder voiding. Of these, 96 patients were scanned using a 3T Biograph mMR Siemens system, employing a gradient echo sequence with inversion recovery preparation. The specific parameters for these MRI scans were: repetition time (TR) of 1900 ms, echo time (TE) of 2.81 ms, a flip angle of 15°, an acquisition matrix of 256 × 256, and single excitations. The remaining 4 patients underwent ^{18}F-FET PET/CT scans on a Biograph 128 Vision 600 Edge scanner. The CT parameters included: 120 kVp, 33 mA, 59 mAs, 1000 ms exposure time, and a 500 mm reconstruction diameter, with images reconstructed using a medium smooth kernel (H38s). Prior to imaging, all 100 patients received an intravenous bolus of 693.8 ± 79.6 MBq (18.7 ± 2.2 mCi) (median: 698.6 MBq, range: 284.9 MBq - 876.9 MBq) of ^{18}F-FET, followed by a saline flush. The PET data were collected continuously from injection to 40 minutes in list mode, allowing retrospective binning for reconstruction of static images over any given time frame. Only the 20-40 minute static frame was used for analysis of TBRs. In 3 patients who could not tolerate full acquisition, a shorter static interval of 27.5-32.5 minutes was used. In all cases included, the shorter acquisition was diagnostic.

Retrospective Imaging Analysis

Following outcome determination of POD or TRC, the static 20-40 minute ^{18}F-FET PET sequence was submitted for a retrospective analysis for lesions of interest volume delineation. The analysis was independently performed by 3 researchers with varying levels of clinical expertise: a board-certified neuroradiologist, an imaging analyst, and a third-year medical student. For each case, the 20-40-minute attenuation-corrected static PET sequence was co-registered with either contrast-enhanced axial T1-weighted MRI or CT to produce fusion images and confirm tumor localization (Figure 1A). All analyses were conducted using a custom workflow in MIM Software® v7.4. Within the workflow, a 1 cm diameter spherical volume of interest (VOI) was first placed within the region of highest PET uptake localized using the SUVmax finder tool (1B), with a corresponding much larger curvilinear VOI placed in the contralateral normal brain to calculate the single voxel tumor-to-background ratio maximum (TBRmax) (Figure 1C). Whole brain TBR maps were then generated, and a second, larger VOI was then placed over the entire area of interest to ensure capture of the highest TBRmax value (1D). The PET/MR fusion is also included for reference. TBRmax volumes were then delineated across the interrogated TBRthres (≥1.6, ≥2.0, ≥2.5, ≥3.0, ≥3.5, ≥ 4.0, ≥4.5, and ≥5.0) (Figure 1E). (This MIM workflow can be made available upon request.)

Data Analysis

To assess inter-rater reliability of capturing TBRthres maps, intraclass correlation coefficients (ICC) were calculated using a 2-way mixed-effect, single-rater model (ICC [3,1]).[44] For each patient, each TBRthres map result was averaged across all 3 raters to generate final volume estimates. The diagnostic performance of both volumetric and single voxel conventional PET metrics in predicting 6-month outcomes was evaluated using receiver operating characteristic (ROC) analysis. The prognostic value of volumetric TBRthres metrics and single-voxel TBRmax was evaluated using Cox proportional hazards regression models. Kaplan–Meier survival analysis was performed by stratifying patients based on a given TBRthres map that exceeded an optimal cutoff determined from ROC curves and compared with patients with a TBRthres map result below these thresholds. To assess incremental predictive value, ROC analyses were performed comparing models based on TBRmax alone versus combined models incorporating both TBRmax and volumetric parameters, with AUCs compared using DeLong's nonparametric test for correlated ROC curves.[45]

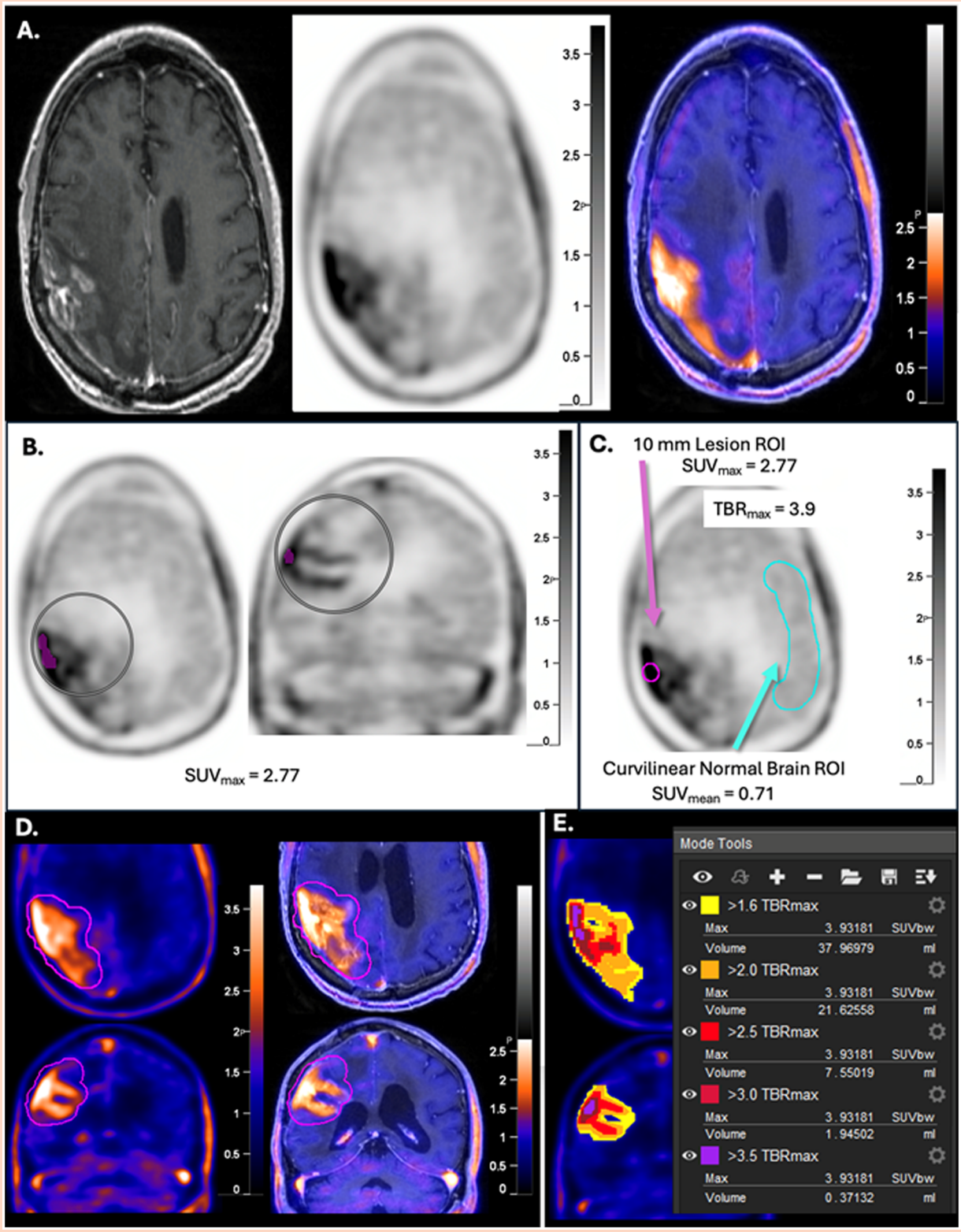

Figure 1. Step-by-step TBRthres MIM Workflow. (A) PET and MR images are imported into the MIM workflow and fused for anatomic guidance. (B) SUVmax is identified within the lesion of interest using the SUVmax finder tool. (C) A 10 mm diameter ROI is placed over the SUVmax region and a larger curvilinear ROI is placed over the contralateral non-diseased brain to estimate normal brain SUVmean. The lesion SUVmax and normal brain SUVmean are used to calculate the tumor-to-brain ratio maximum (TBRmax). (D) A whole-brain TBR map is generated, and a larger 3D volume of interest (VOI) is placed to encompass the lesion. (E) Multiple TBR thresholds are applied to generate corresponding metabolically active tumor volumes.

Results

Demographics

The study population consisted of 100 patients (68 men, 32 women) with primary glioma imaged during clinical care at a single U.S. institution between 2020 and 2023. The patients underwent either ^{18}F-FET PET/MRI (n=96) or ^{18}F-FET PET/CT (n=4, due to MRI contraindications) after surveillant imaging on the immediate prior MRI showed equivocal evidence for POD or TRC. Prior to the FET PET/MRI, all patients received some combination of surgical resection, radiation, or temozolomide and 82 received the Stupp protocol. Therapies prior to ^{18}F-FET PET are summarized in Supplementary Table S5. Most gliomas were supratentorial (n=97) with balanced laterality (left=42, right=58). Summary of patient demographics, tumor characteristics, treatment histories, and clinical outcomes are represented in Table 1.

Table 1. Summary of demographic, tumor, treatment characteristics, and outcomes of 100 primary glioma patients who underwent ^{18}F-FET PET.

Demographics		
Age at FET (years), median (range) (y)		58 (18-77)
	Male/female	68/32
Race/Ethnicity	White/Caucasian	93
	Black/African-American	3
	Hispanic/Latinx	3
	Asian	1
Tumor characteristics		
WHO 2021 Grade/Type	Glioblastoma, IDH-wildtype (WHO Grade 4)	70
	Astrocytoma, IDH-mutant (WHO Grades 2–4)	20
	Oligodendroglioma, IDH-mutant (WHO Grades 2–3)	6
	Other/unspecified	1/3
IDH status (n =96)	Wild type/mutated	73%/27%
MGMT status (n=78)	Unmethylated	50%
	Methylated	43%
	Low level methylation	6%
Treatment history		
Prior interventions	Biopsy only	13
	Resection	87
	Radiation therapy	98
	Chemotherapy	97
	Temozolomide	93
	Lomustine	16
	Bevacizumab	13
	Adjuvant temozolomide cycles, median (mean)	85, 4 (5)
Time from surgery to FET, median (range) (d)		303 (15-5,936)
Time from radiation to FET, median (range) (d)		305 (22-1,899)
Disease outcome and assessment		
Diagnosis of ^{18}F-FET PET	Progression of disease	76
	Treatment-related changes	24
6-month determination	Histology	29
	Clinical follow-up/imaging	71
6-month diagnosis	Progression of disease	76
	Treatment-related changes	24

Reproducibility of Tumor Volumes and TBRmax

In accordance with the emphasis on inter-rater reproducibility in guidelines, the assessment of TBRthres maps demonstrated strong inter-rater reliability across various thresholds among 3 independent readers. Using an Intraclass Correlation Coefficient (ICC (3,1)), agreement was observed for TBR ≥ 1.6 (ICC=0.941, 95% CI, 0.919-0.958), and multivoxel TBR ≥ 5.0 (ICC=0.951, 95% CI, 0.888-0.982), representing the highest concordances within the measured range. Good to excellent reliability was consistently maintained for intermediate TBR thresholds, including multivoxel TBRthres ≥ 2.0 (ICC=0.877, 95% CI, 0.832-0.912), TBRthres ≥ 2.5 (ICC=0.921, 95% CI, 0.888-0.945), TBRthres ≥ 3.0 (ICC=0.931, 95% CI, 0.901-0.954), and TBRthres ≥ 3.5 (ICC=0.920, 95% CI, 0.875-0.951). While a slight trend toward decreased reliability was noted at higher TBR thresholds (TBRthres 4.0: ICC=0.886, 95% CI, 0.800-0.941), overall agreement remained strong. The conventional single-voxel TBRmax measurements also exhibited excellent inter-rater reliability (ICC=0.907, 95% CI, 0.873-0.933).

Inter-reader correlation analysis demonstrated strong agreement for both TBRthres maps and single-voxel TBRmax metrics (Supplementary Figure S1). Individual reader measurements for TBRthres maps at ≥1.6, ≥2.0, and ≥2.5 consistently showed high correlation with the average reader values. This was evidenced by high coefficients of determination (R^2 = 0.960 for TBRthres ≥ 1.6 (Supplementary Figure S1A), 0.917 for TBRthres ≥ 2.0 (Supplementary Figure S1B), and 0.949 for TBRthres ≥ 2.5 (Supplementary Figure S1C). Similarly, single-voxel TBRmax measurements exhibited strong inter-reader correlation (R^2 = 0.935, Supplementary Figure S1D). The precisely estimated linear regression lines and narrow 95% confidence intervals across all panels highlight the reproducibility of these measurements. The insets further confirm this strong agreement, even for smaller lesions and lower TBRthres values. While some variability in individual volume measurements was observed, particularly for larger tumors, TBRthres measurements showed tight concordance with minimal data scatter around the regression line.

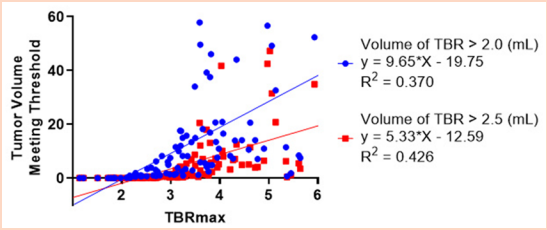

Figure 2. Correlation of single voxel TBRmax with increasing tumor volume. The scatter plot illustrates the correlation between TBRmax and TBRthres. Tumor volumes were quantified based on regions exceeding a TBRthres ≥ 2.0 (circles) and a TBR threshold of 2.5 (squares). Solid lines show the linear regression for each dataset. Each point represents an individual lesion.

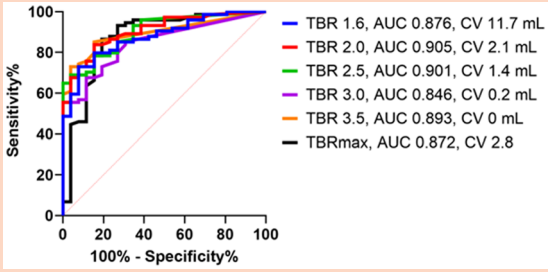

Figure 3. Comparative diagnostic performance of static ^{18}F-FET PET metrics for predicting six-month outcomes in glioma patients. Receiver operating characteristic (ROC) curves illustrate the diagnostic utility of various ^{18}F-FET PET parameters in differentiating POD from TRC at six months post-treatment. The analysis compares tumor volumes defined by varying TBRthres (≥ 1.6, ≥ 2.0, ≥ 2.5, ≥ 3.0, and ≥ 3.5) against single-voxel TBRmax. The plot displays sensitivity versus 100% minus specificity. The diagonal dashed line represents no discrimination (AUC = 0.5). Diagnostic performance is compared across metrics, with the highest accuracy achieved by TBRthres ≥ 2.0.

Correlation of Single-Voxel TBRmax and Tumor Volume

To thoroughly understand the interplay between high tumor activity and the overall extent of active tumor burden, we investigated the correlation between 2 single-voxel TBRmax units (TBRmax > 2.0 and TBRmax > 2.5) and 2 volumetry thresholds (TBRthres > 2.0 and > 2.5) (Figure 2). Consistent with the understanding that the magnitude of radiotracer uptake may correlate with the regional quantity of active tumor cells, single-voxel TBRmax thresholds demonstrated a statistically significant, moderate positive correlation with TBRthres ≥ 2.0 (Pearson's r=0.59, R^2 = 0.37, P<.0001) and ≥ 2.5 (Pearson's r=0.63, R^2 = 0.42, P<.0001). These findings indicate that while higher single voxel TBRmax is associated with larger PET volumes, these metrics capture distinct yet complementary aspects of tumor characteristics. The observed R^2 values, suggesting that single voxel TBRmax accounts for only 35%-40% of the variance in these volume measurements, indicate that each metric provides unique information for comprehensive tumor assessment.

Threshold-Dependent Diagnostic Performance of Single-Voxel-Based TBRmax

To quantitatively assess the diagnostic performance of single voxel TBRmax in distinguishing POD from TRC, threshold-dependent sensitivity and specificity for POD were evaluated across a continuous range of single-voxel TBRmax values (Supplementary Figure S2). As single voxel TBRmax thresholds increased, sensitivity decreased while specificity increased, reflecting an inverse sigmoidal relationship between the 2 measures. At lower thresholds (TBRmax 1.6-1.8), sensitivity was near maximal, but specificity remained below 20%, indicating limited ability to exclude TRC. Specificity improved with increasing thresholds and reached approximately 96% at single voxel TBRmax values ≥ 3.8, though a small number of false positives remained. Nonlinear regression modeling showed strong fits for both sensitivity (R^2 = 0.9992; $IC_{50} \approx 3.5$) and specificity (R^2 = 0.9954; $IC_{50} \approx 2.2$), representing the single voxel TBRmax thresholds at which each metric reached 50% of its respective dynamic range. The point at which sensitivity and specificity most closely converged occurred at single voxel TBRmax 2.9, suggesting this may represent a threshold zone with relatively balanced diagnostic performance under the conditions observed in this cohort.

Diagnostic Performance of Volumetric and Conventional PET Metrics for Six-Month Outcomes

To evaluate the diagnostic utility of TBR metrics in differentiating POD from TRC, we performed ROC analysis with 6-month post-treatment clinical outcomes or pathology as a ground-truth standard (Figure 3). This analysis assessed the predictive ability of various volumetric TBRthres maps and the single-voxel TBRmax. Among all evaluated metrics, the volume delineated by a TBRthres ≥ 2.0 demonstrated the highest diagnostic accuracy, achieving an AUC of 0.905 with an optimal cutoff volume of ≥ 2.1 mL. However, all tested thresholds achieved high accuracy comparable to single-voxel TBRmax at the optimal referenced volumes. After 6-month follow-up or pathologic confirmation, TBRmax FET imaging diagnosis accuracy was 88% for differentiating POD from TRC (4 false-negatives, 8 false-positives). Supplementary Table S3 includes comparative diagnostic performance of FET-PET TBRmax and volumetric TBRthres in predicting 6-month outcome.

Prognostic Significance of Volumetric Tumor Burden

To determine the prognostic significance of various TBRthres maps derived from ^{18}F-FET PET imaging, we conducted Kaplan–Meier survival analyses and Cox proportional hazards modeling. Across all evaluated volumetric thresholds of ≥1.6, ≥2.0, ≥2.5, and ≥3.0, patients with volumes exceeding the respective cutoff values demonstrated significantly reduced overall survival compared to those with subthreshold volumes (Figure 4A-D). The TBRthres ≥ 2.0, using an

optimal cutoff of 2.1 mL, exhibited the strongest prognostic performance. Patients with tumor volumes equal to or greater than 2.1 mL had a median survival of 496 days, whereas the median survival of those with volumes below this threshold was not reached during the follow-up period (> 1728 days) (Figure 4B), indicating a durable survival benefit in the lower-burden group. The Cox model revealed a hazard ratio (HR) of 4.45 (95% CI, 2.16-9.17; P<.0001), reflecting an over 4-fold increased risk of death in patients with higher TBRthres volumes (Supplementary Table S4). Similarly, TBRthres ≥ 1.6 (cutoff 11.7 mL), ≥ 2.5 (cutoff 1.4 mL), and ≥ 3.0 (cutoff 0.16 mL) were each significantly associated with reduced survival, with HRs of 3.59, 3.10, and 3.07, respectively (all P<.001) (Figure 4A, C, D, Supplementary Table S4). In contrast, single-voxel-based TBRmax metrics demonstrated lower prognostic utility. Using a single-voxel TBRmax threshold of ≥2.8, patients with higher values had a median survival of 514 days, whereas those below this threshold survived beyond the study period (MS > 1,728 days) (Figure 4E). The associated HR was 2.30 (95% CI, 1.18-4.47; P=.0143), which, while statistically significant, was lower in magnitude and less discriminatory than the volumetric thresholds (Supplementary Table S4). However, when adjusted using Bonferroni correction, TBRmax 2.8 failed to reach the threshold for statistical significance (P≥.0083). A separate dichotomization at single-voxel TBRmax ≥ 2.5 yielded a median survival of 522 days for the high group and > 1728 days for the low group, with an HR of 2.65 (P=.0114) (Figure 4F).

In univariate Cox analysis (Supplementary Table S5A), all volumetric thresholds demonstrated significant associations with overall survival, whereas TBRmax showed a comparatively lower effect size. However, these findings alone do not establish superiority but rather indicate comparable prognostic capability at the univariate level. To further evaluate independence and potential incremental value, multivariate Cox models were constructed using 2 complementary adjustment strategies (Supplementary Tables S5B and S5C). When adjusted for clinical covariates (age, sex, tumor type, time from surgery to imaging, and chemotherapy exposure), neither volumetric TBRthres metrics nor TBRmax remained statistically significant predictors of overall survival (Supplementary Table

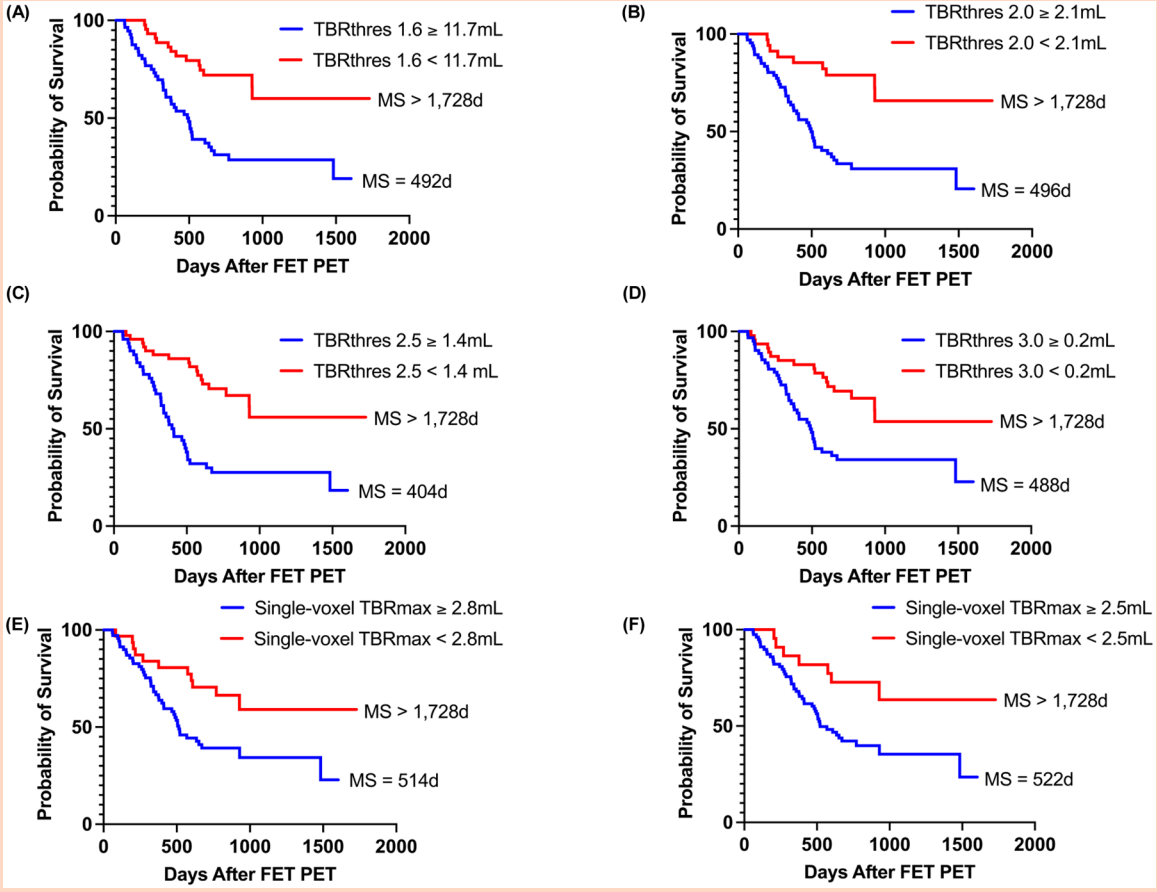

Figure 4. Kaplan-Meier survival analysis based on TBR metrics. Overall survival probability over time is shown for patient cohorts, stratified by optimal thresholds of various TBR metrics (including TBRthres map volumes and single-voxel TBRmax values), all derived from ROC curve analysis presented in Figure 5. (A) Survival curves stratified by the TBRthres ≥ 1.6 volume cutoff (≥11.7 mL vs. < 11.7 mL). (B) Survival curves stratified by the TBRthres ≥ 2.0 volume cutoff (≥2.1 mL vs. <2.1 mL). (C) Survival curves stratified by the TBRthres ≥ 2.5 volume cutoff (≥1.4 mL vs. <1.4 mL). (D) Survival curves stratified by the TBRthres ≥ 3.0 volume cutoff (≥0.2 mL vs. <0.2 mL). (E) Survival curves stratified by the single-voxel TBRmax cutoff (≥2.8 vs. <2.8). (F) Survival curves stratified by the single-voxel TBRmax cutoff (≥2.5 vs. <2.5). *X*-axis, days after ^{18}F-FET PET/MRI or PET/CT diagnosis; *Y*-axis, Probability of Survival; MS, median survival; HR, hazard ratio. Corresponding statistical analysis is presented in Supplementary Table S4.

Table 2. Comparison of predictive performance of AUC for TBRmax alone versus combined models incorporating TBRmax and threshold-specific volumetric ^{18}F-FET PET metrics.

Predictor	AUCTBRmax	AUC combined (TBRmax+TBRthres)	*P*-value
TBRthres ≥ 1.6	0.6155395	0.7000805	.0094013
TBRthres ≥ 2.0	0.6155395	0.7155797	.0193566
TBRthres ≥ 2.5	0.6155395	0.6706924	.0346961
TBRthres ≥ 3.0	0.6155395	0.6797504	.2175744

S5B), indicating that prognostic associations are influenced by underlying clinical factors, as expected. In contrast, in multivariate models adjusting specifically for TBRmax (Supplementary Table S5C), all volumetric TBRthres metrics remained significantly associated with overall survival across thresholds (HR range: 3.19-5.56; $P<.01$). This finding demonstrates that volumetric metrics capture prognostic information that is not fully explained by single-voxel TBRmax, supporting their non-redundant contribution.

To directly test whether volumetric metrics provide incremental predictive value beyond TBRmax, ROC analyses were performed comparing models based on TBRmax alone versus combined models incorporating both TBRmax and volumetric parameters (Table 2). The addition of volumetric metrics resulted in a statistically significant improvement in predictive performance at selected thresholds. Specifically, inclusion of TBRthres ≥ 1.6 (volume cutoff 11.7 mL) increased AUC from 0.62 to 0.70 ($P=.009$), while TBRthres ≥ 2.0 (volume cutoff 2.1 mL) increased AUC from 0.62 to 0.72 ($P=.019$). TBRthres ≥ 2.5 (volume cutoff 1.4 mL) yielded a smaller but statistically significant improvement (AUC 0.62 to 0.67, $P=.035$) (Table 2). In contrast, TBRthres ≥ 3.0 (volume cutoff 0.16 mL) did not demonstrate a statistically significant improvement (AUC 0.62 to 0.68, $P=.218$) (Table 2). Collectively, these findings suggest that volumetric TBRthres metrics may provide complementary prognostic information to TBRmax at selected thresholds, although the magnitude of improvement varied across thresholds.

Discussion

AA PET is increasingly being incorporated into clinical practice in various countries[21,46] and, recently, the PET-based response assessment criteria for diffuse gliomas (RANO-PET 1.0) was published for inclusion of AA PET into clinical trials.[37] Within RANO-PET 1.0 an important component of response assessment is the inclusion of percent change in PET-based tumor volume. In addition, studies have shown that AA PET volumes often exceed the volume of contrast enhancement.[47] Finally, it was already shown that glioma resection using ^{18}F-FET PET is significantly correlated with improved prognosis.[48] Despite this, few studies have performed a thorough assessment of volumes derived from various TBR thresholds. Therefore, the aim of this study was to determine to what degree volumetric ^{18}F-FET PET TBRthres metrics can provide clinically useful information in a quantitative manner in patients with primary malignant glioma within a range of treatment regimens and timelines as often encountered in the clinical care domain. For these cases, complementary TBRthres mapping improved clinical confidence in recognizing POD from TRC. Overall, consistent among readers of varying expertise, provide parallel value in delineating POD from TRC, are not highly correlated with single-voxel TBRmax values, and carry potentially important prognostic value.

The first question we studied was the degree to which TBRthres maps could be constructed using readily available clinical software and a simple workflow that could be feasibly implemented without nuclear medicine credentialing (Neuroradiologist, imaging analyst, and medical student). The inter-rater reliability analysis demonstrated reproducibility across 3 independent researchers of varying clinical experience across all TBRthres volumes from ≥1.6 through ≥5.0 (ICC > 0.86). These findings suggest that manual volumetric workflow is reasonably reproducible across readers with varying clinical expertise. Notably, inter-rater reliability reached ICC of 0.951 for TBRthres ≥ 5.0, and 0.941 for TBRthres ≥ 1.6, demonstrating good concordance even at the lowest and highest measured TBRthres volumes. Furthermore, a strong linear correlation between individual reader measurements and averaged values for both TBRthres and single-voxel TBRmax highlights the strength of the volumetric analysis method across different readers. The average time to completion of the workflow was approximately 5 minutes, including manual VOI selection of the tumor region of interest and contralateral control region. The simple criteria used in this workflow indicate that an automated or semi-automated analytic tool can be developed to reduce analysis time while maintaining reproducibility of the technique which will be the focus of future work.

The second question assessed was the relationship between single-voxel TBRmax and TBRthres maps of the same cutoff. Although higher single-voxel TBRmax values were significantly correlated with larger TBRthres volumes, this metric explained only 35%-40% of the variance, indicating that these measures reflect overlapping but fundamentally distinct biological features. The remaining 60%-65% of unexplained variance likely arises from tumor-intrinsic factors not captured by a single point of peak uptake, such as histological grade, molecular subtype, spatial heterogeneity in cellularity and metabolism, and microenvironmental influences, including hypoxia, necrosis, and vascular architecture. This divergence is biologically and clinically meaningful: while single-voxel TBRmax helps localize the "hotspot" (for a voxel whose size may actually be smaller than the volumetric resolution of the camera), it may fall short in representing the full spatial complexity and burden of disease. In contrast, TBRthres maps may assist with providing a more integrated view of tumor extent and heterogeneity. This discrepancy reinforces the need for multi-parametric imaging in glioma assessment,[49,50] where reliance on a single voxel-based metric risks oversimplifying complex disease biology.

In primary glioma assessment, "borderline cases" pose an uncertainty in evaluating tumor relapse from nonspecific treatment changes. Therefore, the third question focused on diagnostic performance: specifically, how different values of single-voxel TBRmax thresholds affect the sensitivity and specificity for distinguishing POD from TRC, particularly in

"borderline" or equivocal cases. Using a relatively homogeneous imaging dataset (N=96 scans) from a cohort of 100 patients, we found that the optimal diagnostic performance was achieved at single-voxel TBRmax thresholds between 2.3 and 2.6, marking an optimal clinical decision-making window where the tradeoff between early detection and diagnostic confidence is most effectively balanced. However, diagnostic accuracy remained imperfect, especially within a broader diagnostic window ranging from 1.8 to 3.8, reflecting the intrinsic limitations of relying solely on single-voxel TBRmax for dichotomous clinical decisions. These findings highlight the need to consider other image analysis metrics, such as volumes at given threshold to refine discrimination between POD and TRC and enhance the confidence of clinical decision making.

Our study demonstrates that volumetric ^{18}F-FET PET TBRthres metrics provide reproducible and clinically interpretable measures of tumor burden, with prognostic associations comparable to those obtained using single-voxel TBRmax. Although our original hypothesis proposed that volumetric metrics would demonstrate superior diagnostic and prognostic utility compared with TBRmax alone, the present findings instead support a more nuanced interpretation. Specifically, volumetric metrics showed largely comparable standalone performance but provided modest, threshold-dependent incremental prognostic value when combined with TBRmax, supporting a complementary rather than universally superior role.

Importantly, our results clarify that volumetric metrics should not be interpreted as universally superior to TBRmax, but rather as complementary measures that capture distinct aspects of tumor biology. At the univariate level, both volumetric and single-voxel metrics demonstrated significant associations with survival, showing prognostic relevance of amino acid PET-derived metrics, including TBRmax and volumetric parameters. However, such comparisons do not address whether these metrics provide overlapping or independent information. To address this, we performed multivariate analyses using 2 distinct adjustment strategies. When adjusted for clinical covariates, neither volumetric metrics nor TBRmax remained statistically significant predictors, indicating that both imaging-derived measures are influenced by underlying patient and disease characteristics. This finding highlights the importance of interpreting imaging biomarkers within the broader clinical context. In contrast, when adjusting specifically for TBRmax, volumetric TBRthres metrics remained significantly associated with overall survival across all evaluated thresholds. This demonstrates that volumetric parameters capture prognostic information that is not fully represented by single-voxel intensity measures, supporting a non-redundant biological contribution. To directly evaluate incremental value, we compared predictive models based on TBRmax alone versus combined models incorporating volumetric parameters. These analyses revealed that volumetric metrics provided statistically significant improvements in predictive performance at selected thresholds, particularly TBRthres ≥ 1.6 and ≥ 2.0, with smaller improvement observed at TBRthres ≥ 2.5, while no significant improvement was identified at TBRthres ≥ 3.0. This threshold-dependent pattern suggests that intermediate volumetric thresholds may better capture clinically relevant metabolically active tumor burden than either very low or highly restrictive thresholds. However, the observed improvements in predictive performance were modest and should be interpreted cautiously given the retrospective single-institution design and limited sample size. This threshold-dependent effect is a key finding and explains why volumetric metrics may appear equivalent to TBRmax when evaluated in isolation. From a biological perspective, this distinction is plausible. Single-voxel TBRmax reflects the point of maximal tracer uptake, whereas volumetric TBRthres maps incorporate the spatial extent of metabolically active tumor. The moderate correlation observed between these measures ($R^2 \approx 0.35$-0.40) further supports that they capture overlapping but distinct features of tumor biology. From a clinical standpoint, these findings suggest that volumetric PET metrics may provide added value in specific contexts, particularly when optimized thresholds are applied, rather than serving as a universal replacement for TBRmax. Given the additional time and complexity required for volumetric analysis, its routine implementation should be guided by demonstrated incremental benefit, as observed in selected thresholds in this study. Taken together, our results support a model in which volumetric and single-voxel PET metrics provide complementary, partially independent information, with incremental prognostic value that is dependent on threshold selection and clinical context.

Several limitations of this study warrant discussion. First, despite high reproducibility, TBRthres associated volumes are inherently sensitive to the placement of contralateral reference regions, which may introduce variability, particularly in cases with asymmetric background uptake or underlying white matter abnormalities. Utilizing minimum TBRthres volumes (ie the oft cited 1.6 mm^2 area) rather than single voxels for reference uptake estimation may help mitigate this issue. Second, this was a retrospective study conducted at a single institution using uniform imaging protocols that routinely apply single voxel TBRmax and TBRmean values to the final report, which may limit generalizability. Further prospective validation studies are needed to confirm and refine the diagnostic and prognostic utility of these volumetric PET thresholds. Third, while we focused on TBR thresholds and volumes, integration with molecular and histopathological features, such as isocitrate dehydrogenase mutation status or O-6-methylguanine-DNA methyltransferase promoter methylation may further refine predictive modeling. Additionally, relying on clinical judgment as the gold standard introduces subjectivity into outcome assessment, as the ground truth relies on multifactorial data rather than an absolute measure. Even pathologic analysis is not always as straightforward as a gold standard.[51,52] If a patient had the lesion surgically resected (or) underwent other treatment changes after the PET, this could have contributed to improved overall survival in some cases. This limitation is inherited from the clinical care domain. Finally, as volumetric analysis becomes more integrated into clinical practice, developing validated automated tools and image harmonization protocols will be critical to minimize operator dependence and enhance reproducibility across institutions.

Conclusion

Threshold-based volumetric analysis of ^{18}F-FET PET provides a reproducible measure of metabolically active tumor

burden and demonstrates diagnostic and prognostic performance comparable to single-voxel TBRmax. Volumetric TBRthres metrics capture complementary information that is not fully reflected by TBRmax and, at selected thresholds, provide modest incremental predictive information for mortality risk stratification. However, this added value is not uniform across thresholds and is attenuated after adjustment for clinical covariates, indicating context-dependent utility. These findings support further investigation of volumetric PET metrics, particularly when integrated with TBRmax using clinically relevant thresholds, to better define their role in clinical decision-making for glioma patients.

Supplementary Material

Supplementary material is available *online at Neuro-Oncology Advances* (https://academic.oup.com/noa).

Keywords

^{18}F-FET | brain tumor | glioma | imaging | PET

Author Contributions

Contributed significantly to the experimental design: Brian D. Graner, Gary D. Hutchins, Mark A. Green, Philipp Lohmann, and Michael C. Veronesi. Contributed significantly to the experiment implementation: Thura Tun Oo, Shaun D. Grega, Nathaniel J. Smith, Sharon Sidenbender, Jesus A. Ocana, Matthew E. Larson, Mark Tann, Kathryn Nevel, Brian D. Graner, Philipp Lohmann, and Michael C. Veronesi. Contributed significantly to the analysis and interpretation of the data: Thura Tun Oo, Shaun D. Grega, Nathaniel J. Smith, Lu Mao, Tristan K. Deaton, Keith G. Ciantar, Wendy Territo, Sharon Sidenbender, Kathryn Nevel, Brian D. Graner, Gary D. Hutchins, Mark A. Green, Philipp Lohmann, Michael C. Veronesi. All authors were involved in the writing of the manuscript at draft and any revision stages and have read and approved the final version.

Conflict of Interest Statement

M.C.V. and P.L. have received honorarium for paid speakerships and advisory board participation with Telix Pharmaceuticals. M.C.V., M.T., M.A.G., and P.L. have/had research contracts with Telix Pharmaceuticals. M.C.V., J.A.O., and B.D.G. have received salary coverage for research projects associated with Telix Pharmaceuticals. T.T.O.'s Post-doctoral fellow salary is funded through other research projects associated with Telix Pharmaceuticals. None is declared for the remainder of the authors.

Funding

K.G.C. and P.L. received funding by the Deutsche Forschungsgemeinschaft (DFG, German Research Foundation)—Projektnummer(n) 428090865/SPP2177. No other author utilized funding for the purpose of the research study.

Acknowledgments

The authors gratefully acknowledge the contribution made by these patients through their consent to the use of their deidentified imaging findings and clinical records in retrospective research.

Ethics Approval Statement

The Indiana University Institutional Review Board reviewed and approved the study and informed consent was obtained from the subjects in person prior to commencing with the imaging who expressed understanding that the results of the imaging would be used for future research in a de-identified and HIPPA compliant manner.

Data Availability

The data will be made available upon reasonable request which is stored in excel format and was analyzed using the graph pad statistical program.

Affiliations

School of Medicine and Public Health, University of Wisconsin, Madison, Wisconsin, USA (T.T.O., L.M., M.E.L., M.C.V.); Indiana University School of Medicine, Indianapolis, Indiana, USA (S.D.G., N.J.S., T.K.D., W.T., S.S., J.A.O., M.T., K.N., B.D.G., G.D.H., M.A.G.); Institute of Neuroscience and Medicine (INM-3, INM-4), Research Center Juelich, Juelich, Germany (K.G.C., P.L.); Department of Nuclear Medicine, RWTH Aachen University Hospital, Aachen, Germany (P.L.)

References

1. Galldiks N, Lohmann P, Aboian M, et al. Update to the RANO working group and EANO recommendations for the clinical use of PET imaging in gliomas. *Lancet Oncol*. 2025;26:e436-e447. https://doi.org/10.1016/S1470-2045(25)00193-7

2. Galldiks N, Lohmann P, Albert NL, Tonn JC, Langen K-J. Current status of PET imaging in neuro-oncology. *Neurooncol Adv*. 2019;1:vdz010. https://doi.org/10.1093/noajnl/vdz010
3. Harat M, Rakowska J, Harat M, et al. Combining amino acid PET and MRI imaging increases accuracy to define malignant areas in adult glioma. *Nat Commun*. 2023;14:4572. https://doi.org/10.1038/s41467-023-39731-8
4. Singnurkar A, Poon R, Detsky J. 18F-FET-PET imaging in high-grade gliomas and brain metastases: a systematic review and meta-analysis. *J Neurooncol*. 2023;161:1-12. https://doi.org/10.1007/s11060-022-04201-6
5. Maurer GD, Brucker DP, Stoffels G, et al. (18)F-FET PET imaging in differentiating glioma progression from treatment-related changes: a single-center experience. *J Nucl Med*. 2020;61:505-511. https://doi.org/10.2967/jnumed.119.234757
6. Pöpperl G, Kreth FW, Herms J, et al. Analysis of 18F-FET PET for grading of recurrent gliomas: is evaluation of uptake kinetics superior to standard methods? *J Nucl Med*. 2006;47:393-403.
7. Galldiks N, Stoffels G, Filss C, et al. The use of dynamic O-(2-18F-fluoroethyl)-l-tyrosine PET in the diagnosis of patients with progressive and recurrent glioma. *Neuro Oncol*. 2015;17:1293-1300. https://doi.org/10.1093/neuonc/nov088
8. Robert JA, Leclerc A, Ducloie M, Emery E, Agostini D, Vigne J. Contribution of [(18)F]FET PET in the management of gliomas, from diagnosis to follow-up: a review. *Pharmaceuticals (Basel)*. 2024;17:1228. https://doi.org/10.3390/ph17091228
9. Wester HJ, Herz M, Weber W, et al. Synthesis and radiopharmacology of O-(2-[18F]fluoroethyl)-L-Tyrosine for tumor imaging. *J Nucl Med*. 1999;40:205-212.
10. Galldiks N, Stoffels G, Filss CP, et al. Role of O-(2-(18)F-fluoroethyl)-L-tyrosine PET for differentiation of local recurrent brain metastasis from radiation necrosis. *J Nucl Med*. 2012;53:1367-1374. https://doi.org/10.2967/jnumed.112.103325
11. Ceccon G, Lohmann P, Stoffels G, et al. Dynamic O-(2-18F-fluoroethyl)-L-tyrosine positron emission tomography differentiates brain metastasis recurrence from radiation injury after radiotherapy. *Neuro Oncol*. 2017;19:281-288.
12. Vander Borght T, Asenbaum S, Bartenstein P, et al.; European Association of Nuclear Medicine (EANM). EANM procedure guidelines for brain tumour imaging using labelled amino acid analogues. *Eur J Nucl Med Mol Imaging*. 2006;33:1374-1380. https://doi.org/10.1007/s00259-006-0206-3
13. Kobayashi K, Ohnishi A, Promsuk J, et al. Enhanced tumor growth elicited by L-type amino acid transporter 1 in human malignant glioma cells. *Neurosurgery*. 2008;62:493-503. https://doi.org/10.1227/01.neu.0000316018.51292.19
14. Nawashiro H, Otani N, Shinomiya N, et al. L-type amino acid transporter 1 as a potential molecular target in human astrocytic tumors. *Int J Cancer*. 2006;119:484-492. https://doi.org/10.1002/ijc.21866
15. Galldiks N, Lohmann P, Fink GR, Langen K-J. Amino acid PET in neuro-oncology. *J Nucl Med*. 2023;64:693-700. https://doi.org/10.2967/jnumed.122.264859
16. Werner JM, Tomasich E, Mair MJ, et al. Lack of LAT1 and CD98hc expression on tumor cells of diffuse glioma: revisiting the molecular basis for amino acid PET imaging and theranostics. *J Nucl Med*. 2026. https://doi.org/10.2967/jnumed.125.271348
17. Aoki M, Watabe T, Nagamori S, et al. Distribution of LAT1-targeting PET tracer was independent of the tumor blood flow in rat xenograft models of C6 glioma and MIA PaCa-2. *Ann Nucl Med*. 2019;33:394-403. https://doi.org/10.1007/s12149-019-01346-9
18. Nowosielski M, DiFranco MD, Putzer D, et al. An intra-individual comparison of MRI, [18F]-FET and [18F]-FLT PET in patients with high-grade gliomas. *PLoS One*. 2014;9:e95830. https://doi.org/10.1371/journal.pone.0095830
19. Song S, Cheng Y, Ma J, et al. Simultaneous FET-PET and contrast-enhanced MRI based on hybrid PET/MR improves delineation of tumor spatial biodistribution in gliomas: a biopsy validation study. *Eur J Nucl Med Mol Imaging*. 2020;47:1458-1467. https://doi.org/10.1007/s00259-019-04656-2
20. Ponisio MR, McConathy JE, Dahiya SM, et al. Dynamic (18)F-FDOPA-PET/MRI for the preoperative evaluation of gliomas: correlation with stereotactic histopathology. *Neurooncol Pract*. 2020;7:656-667. https://doi.org/10.1093/nop/npaa044
21. Smith NJ, Deaton TK, Territo W, et al. Hybrid 18F-Fluoroethyltyrosine PET and MRI with perfusion to distinguish disease progression from treatment-related change in malignant brain tumors: the quest to beat the toughest cases. *J Nucl Med*. 2023;64:1087-1092. https://doi.org/10.2967/jnumed.122.265149
22. Law I, Albert NL, Arbizu J, et al. Joint EANM/EANO/RANO practice guidelines/SNMMI procedure standards for imaging of gliomas using PET with radiolabelled amino acids and [(18)F]FDG: version 1.0. *Eur J Nucl Med Mol Imaging*. 2019;46:540-557. https://doi.org/10.1007/s00259-018-4207-9
23. Langen KJ, Stoffels G, Filss CP, et al. Borderline findings in O-(2-[(18)F]-fluoroethyl)-l-tyrosine PET of patients with suspected glioma relapse: role in clinical practice. *J Nucl Med*. 2025;66:187-193. https://doi.org/10.2967/jnumed.124.268768
24. Huttunen J, Peltokangas S, Gynther M, et al. l-type amino acid transporter 1 (LAT1/Lat1)-utilizing prodrugs can improve the delivery of drugs into neurons, astrocytes and microglia. *Sci Rep*. 2019;9:12860. https://doi.org/10.1038/s41598-019-49009-z
25. Gynther M, Puris E, Peltokangas S, et al. Alzheimer's disease phenotype or inflammatory insult does not alter function of L-Type amino acid transporter 1 in mouse blood-brain barrier and primary astrocytes. *Pharm Res*. 2018;36:17. https://doi.org/10.1007/s11095-018-2546-7
26. Suehiro JI, Kimura T, Fukutomi T, et al. Endothelial cell-specific LAT1 ablation normalizes tumor vasculature. *JCI Insight*. 2024;9:e171371. https://doi.org/10.1172/jci.insight.171371
27. Cai L, Kirchleitner SV, Zhao D, et al. Glioblastoma exhibits inter-individual heterogeneity of TSPO and LAT1 expression in neoplastic and parenchymal cells. *Int J Mol Sci*. 2020;21:612. https://doi.org/10.3390/ijms21020612
28. Bashir A, Mathilde Jacobsen S, Mølby Henriksen O, et al. Recurrent glioblastoma versus late posttreatment changes: diagnostic accuracy of O-(2-[18F]fluoroethyl)-L-tyrosine positron emission tomography (18F-FET PET). *Neuro Oncol*. 2019;21:1595-1606. https://doi.org/10.1093/neuonc/noz166
29. Vettermann FJ, Diekmann C, Weidner L, et al. L-type amino acid transporter (LAT) 1 expression in (18)F-FET-negative gliomas. *EJNMMI Res*. 2021;11:124. https://doi.org/10.1186/s13550-021-00865-9
30. Floeth FW, Pauleit D, Sabel M, et al. 18F-FET PET differentiation of ring-enhancing brain lesions. *J Nucl Med*. 2006;47:776-782.
31. Hutterer M, Nowosielski M, Putzer D, et al. [18F]-fluoro-ethyl-L-tyrosine PET: a valuable diagnostic tool in neuro-oncology, but not all that glitters is glioma. *Neuro Oncol*. 2013;15:341-351. https://doi.org/10.1093/neuonc/nos300
32. Kido Y, Tamai I, Uchino H, Suzuki F, Sai Y, Tsuji A. Molecular and functional identification of large neutral amino acid transporters LAT1 and LAT2 and their pharmacological relevance at the blood-brain barrier. *J Pharm Pharmacol*. 2001;53:497-503. https://doi.org/10.1211/0022357011775794

33. Nakada N, Mikami T, Hana K, et al. Unique and selective expression of L-amino acid transporter 1 in human tissue as well as being an aspect of oncofetal protein. *Histol Histopathol*. 2014;29:217-227.
34. Gong K, Cherry SR, Qi J. On the assessment of spatial resolution of PET systems with iterative image reconstruction. *Phys Med Biol*. 2016;61:N193-N202. https://doi.org/10.1088/0031-9155/61/5/N193
35. Filss CP, Albert NL, Böning G, et al. O-(2-[(18)F]fluoroethyl)-L-tyrosine PET in gliomas: influence of data processing in different centres. *EJNMMI Res*. 2017;7:64. https://doi.org/10.1186/s13550-017-0316-x
36. Albert NL, Preusser M. Measure what is measurable: PET RANO 1.0 criteria for interpretation of amino acid PET of diffuse gliomas. *Neuro Oncol*. 2024;26:401-402. https://doi.org/10.1093/neuonc/noad228
37. Albert NL, Galldiks N, Ellingson BM, et al. PET-based response assessment criteria for diffuse gliomas (PET RANO 1.0): a report of the RANO group. *Lancet Oncol*. 2024;25:e29-e41. https://doi.org/10.1016/S1470-2045(23)00525-9
38. Rosen J, Stoffels G, Lohmann P, et al. Prognostic value of pre-irradiation FET PET in patients with not completely resectable IDH-wildtype glioma and minimal or absent contrast enhancement. *Sci Rep*. 2021;11:20828. https://doi.org/10.1038/s41598-021-00193-x
39. Jansen NL, Suchorska B, Wenter V, et al. Prognostic significance of dynamic 18F-FET PET in newly diagnosed astrocytic high-grade glioma. *J Nucl Med*. 2015;56:9-15. https://doi.org/10.2967/jnumed.114.144675
40. Moller S, Law I, Munck Af Rosenschold P, et al. Prognostic value of (18)F-FET PET imaging in re-irradiation of high-grade glioma: Results of a phase I clinical trial. *Radiother Oncol*. 2016;121:132-137. https://doi.org/10.1016/j.radonc.2016.08.014
41. Celli M, Caroli P, Amadori E, et al. Diagnostic and prognostic potential of (18)F-FET PET in the differential diagnosis of glioma recurrence and treatment-induced changes after chemoradiation therapy. *Front Oncol*. 2021;11:721821. https://doi.org/10.3389/fonc.2021.721821
42. Floeth FW, Pauleit D, Wittsack H-J, et al. Multimodal metabolic imaging of cerebral gliomas: positron emission tomography with [18F] fluoroethyl-l-tyrosine and magnetic resonance spectroscopy. *J Neurosurg*. 2005;102:318-327. https://doi.org/10.3171/jns.2005.102.2.0318
43. Bashir A, Brennum J, Broholm H, Law I. The diagnostic accuracy of detecting malignant transformation of low-grade glioma using O-(2-[18F] fluoroethyl)-l-tyrosine positron emission tomography: a retrospective study. *J Neurosurg*. 2018;130:451-464. https://doi.org/10.3171/2017.8.JNS171577
44. Shrout PE, Fleiss JL. Intraclass correlations: uses in assessing rater reliability. *Psychol Bull*. 1979;86:420-428. https://doi.org/10.1037//0033-2909.86.2.420
45. DeLong ER, DeLong DM, Clarke-Pearson DL. Comparing the areas under two or more correlated receiver operating characteristic curves: a nonparametric approach. *Biometrics*. 1988;44:837-845.
46. Heinzel A, Dedic D, Galldiks N, et al. Two decades of brain tumour imaging with O-(2-[(18)F]fluoroethyl)-L-tyrosine PET: the forschungszentrum jülich experience. *Cancers (Basel)*. 2022;14:3336. https://doi.org/10.3390/cancers14143336
47. Lohmann P, Stavrinou P, Lipke K, et al. FET PET reveals considerable spatial differences in tumour burden compared to conventional MRI in newly diagnosed glioblastoma. *Eur J Nucl Med Mol Imaging*. 2019;46:591-602. https://doi.org/10.1007/s00259-018-4188-8
48. Ort J, Hamou HA, Kernbach JM, et al. (18)F-FET-PET-guided gross total resection improves overall survival in patients with WHO grade III/IV glioma: moving towards a multimodal imaging-guided resection. *J Neurooncol*. 2021;155:71-80. https://doi.org/10.1007/s11060-021-03844-1
49. Ellingson BM, Yao J, Raymond C, et al. Multiparametric MR-PET imaging predicts pharmacokinetics and clinical response to GDC-0084 in patients with recurrent high-grade glioma. *Clin Cancer Res*. 2020;26:3135-3144. https://doi.org/10.1158/1078-0432.CCR-19-3817
50. Kim D, Lee SH, Hwang HS, Kim SJ, Yun M. Recent update on PET/CT radiotracers for imaging cerebral glioma. *Nucl Med Mol Imaging*. 2024;58:237-245. https://doi.org/10.1007/s13139-024-00847-4
51. Komori T. Grading of adult diffuse gliomas according to the 2021 WHO classification of tumors of the central nervous system. *Lab Invest*. 2022;102:126-133. https://doi.org/10.1038/s41374-021-00667-6
52. van den Bent MJ. Interobserver variation of the histopathological diagnosis in clinical trials on glioma: a clinician's perspective. *Acta Neuropathol*. 2010;120:297-304. https://doi.org/10.1007/s00401-010-0725-7

 Neuro-Oncology Advances 2026 8(1) 1–12
https://doi.org/10.1093/noajnl/vdag159
Clinical Investigations